Aquaculture 519 (2020) 734797

Contents lists available at ScienceDirect

Aquaculture

journal homepage: www.elsevier.com/locate/aquaculture

Identification of two novel C-type lectins involved in immune defense against white spot syndrome virus and *Vibrio parahaemolyticus* from *Marsupenaeus japonicus*

Jinbin Zheng[a], Yong Mao[b,c,*], Yongquan Su[c], Jun Wang[c]

[a] School of Marine Sciences, Ningbo University, Ningbo 315211, China
[b] State Key Laboratory of Marine Environmental Science, Xiamen University, Xiamen 361102, China
[c] College of Ocean and Earth Sciences, Xiamen University, Xiamen 361102, China

ARTICLE INFO

Keywords:
Marsupenaeus japonicus
C-type lectin
White spot syndrome virus
Vibrio parahaemolyticus

ABSTRACT

C-type lectins (CTLs) are vital molecules in crustacean innate immunity with the capacity to recognize and eliminate invaders, such as viruses and bacteria. Here, two novel CTLs were identified from the kuruma shrimp *Marsupenaeus japonicus*, and their molecular characteristics and immune function were investigated. Sequence analysis revealed that the two CTLs possessed the typical CTL structure and function features. Tissue distribution analysis showed that the two CTLs were most abundantly expressed in the hepatopancreas and weakly expressed in other examined tissues. The transcription of the two CTLs significantly increased in the hepatopancreas of shrimp challenged with both white spot syndrome virus (WSSV) and *Vibrio parahaemolyticus*, and MjCTL4 was found to be more sensitive to the two pathogens than MjCTL3, being induced at relatively faster and higher increments. GST pull-down assays showed that the two CTLs could directly interact with several WSSV envelope proteins (VP19, VP24, VP26 and VP28). Moreover, the two CTLs displayed obvious binding and antibacterial ability to *V. parahaemolyticus*, and MjCTL3 exhibited stronger anti-*V. parahaemolyticus* activity than MjCTL4. These results suggest that the two novel CTLs might function as pattern recognition receptors (PRRs) and antibacterial molecules in *M. japonicus* innate immunity, and the two CTLs may be alternative agents for the prevention and treatment of diseases caused by WSSV and *V. parahaemolyticus*.

1. Introduction

Shrimp farming is one of the most flourishing industries in aquaculture that has generated tremendous economic benefits. In the recent decade (2008–2017), the annual production of cultured shrimp in the world successively increased from 3.40 to 5.51 million tons with a value elevated from 15.11 to 34.22 billion USA dollars (Food and Agriculture Organization of the United Nations Global Production Statistics, 2019). Despite the thriving development of the shrimp farming industry, shrimp aquaculture has been seriously hampered by diseases caused by viruses, bacteria, fungi and protozoa, among which the viruses and bacteria are major causative agents of infectious diseases in shrimp (Manilal et al., 2010; Lightner, 2011; Flegel, 2012; Lightner et al., 2012; Karunasagar and Ababouch, 2012; Thitamadee et al., 2016; Shinn et al., 2018). Among the viroses and bacterioses of cultured shrimp, the white spot syndrome (WSS) and vibriosis caused by white spot syndrome virus (WSSV) and *Vibrio parahaemolyticus*, respectively, have been the most problematic to manage and have been responsible for the most costly epizootics (Kumar et al., 2014; Joshi et al., 2014; Verbruggen et al., 2016; Oakey and Smith, 2018). Although massive efforts have been made, including improved culture practices, routine sanitation and the use of chemotherapeutics and antibiotics, there are still no effective methods to thoroughly control and cure the two severe diseases. Meanwhile, the abuse of antibiotics in shrimp culture with the attempt to control bacterial disease have resulted in serious antibiotics and antibiotic resistance gene contamination, which pose serious threats to the ecological environment and human health (Holmström et al., 2003; Vignesh et al., 2011; Thuy and Loan, 2011; Cabello et al., 2016; Su et al., 2017). Thus, there is an intense desire for exploring environmentally friendly and effective prophylaxis and treatment for diseases caused by WSSV and *V. parahaemolyticus*.

Lectins are a large family of pattern recognition receptors (PRRs) found in almost all metazoans that trigger innate immunity by recognizing and binding to pathogen-associated molecular patterns

* Corresponding author at: College of Ocean and Earth Sciences, Xiamen University, South Xiangan Road, 361102 Xiamen, China.
E-mail address: maoyong@xmu.edu.cn (Y. Mao).

https://doi.org/10.1016/j.aquaculture.2019.734797
Received 18 July 2019; Received in revised form 19 September 2019; Accepted 29 November 2019
Available online 29 November 2019
0044-8486/

Table 1
Primer sequences used in the present study.

Primer name	Primer sequence (5′-3′)	Target
MjCTL3-F	TGAATCCGCCAGCCAAAG	cDNA fragment
MjCTL3-R	GAATCGCCGAAGAAGAAGTG	cDNA fragment
MjCTL4-F	TTTCACCAGGACCAGAGTAT	cDNA fragment
MjCTL4-R	CATCAAGCAGTAGGCAGTTC	cDNA fragment
MjCTL3–3′-Outer	GGATTTCACAACATTGCCGA	3′-RACE PCR
MjCTL3–3′-Inner	ACGGAACGGAGGTCAAGATG	3′-RACE PCR
MjCTL4–3′-Outer	CAAGGCTACGAGGGTGACTG	3′-RACE PCR
MjCTL4–3′-Inner	AGGCGGCACTGAAGAGAACT	3′-RACE PCR
MjCTL3–5′-Outer	CATCTTGACCTCCGTTCCGT	5′-RACE PCR
MjCTL3–5′-Inner	GTCGGCAATGTTGTGAAATCC	5′-RACE PCR
MjCTL4–5′-Outer	AACCAGTCACCCTCGTAGCCT	5′-RACE PCR
MjCTL4–5′-Inner	CATCCTCCCAGGGCATACTC	5′-RACE PCR
MjCTL3-RT-F	TACAGATGGACGGACGGAACG	qRT-PCR
MjCTL3-RT-R	TTGAATCGCCGAAGAAGAAGT	qRT-PCR
MjCTL4-RT-F	TCACCAGGACCAGAGTATGCC	qRT-PCR
MjCTL4-RT-R	CAGCCAGTAAGAGCCAGAAAGA	qRT-PCR
EF1-α-F	GGAACTGGAGGCAGGACC	qRT-PCR
EF1-α-R	AGCCACCGTTTGCTTCAT	qRT-PCR
His-CRD3-F	CCGGAATTCTGCCCCGAAGGATTTCACA	Protein expression
His-CRD3-R	CCCAAGCTTTTACTCACAAATGGCGGAATAATCAG	Protein expression
His-CRD4-F	CCGGAATTCTGTCCTGATGGCTGGCTGG	Protein expression
His-CRD4-R	CCCAAGCTTTTACATACAGAGTGGATGATGAATCAAAT	Protein expression
GST-VP19-F	CGCGGATCCATGGCCACCACGACTAACAC	Protein expression
GST-VP19-R	CCGGAATTCTTATCCCTGGTCCTGTTCTTATATT	Protein expression
GST-VP24-F	CGCGGATCCAACATAGAACTTAACAAGAAATTGGAC	Protein expression
GST-VP24-R	CCGGAATTCTTATTTTTCCCCAACCTTAAACA	Protein expression
GST-VP26-F	CGCGGATCCACACGTGTTGGAAGAAGCGT	Protein expression
GST-VP26-R	CCGGAATTCTTACTTCTTCTTGATTTCGTCCTTG	Protein expression
GST-VP28-F	CGCGGATCCATGGATCTTTCTTTCACTCTTTCG	Protein expression
GST-VP28-R	CCGGAATTCTTACTCGGTCTCAGTGCCAGAG	Protein expression

(PAMPs) in pathogens (Kennedy et al., 1995; Marques and Barracco, 2000; Dam and Brewer, 2009; Vazquez et al., 2009). Based on structural features, carbohydrate specificities and biological functions, lectins identified in shrimp have been divided into several subgroups, including the C-type, L-type, P-type, M-type and fibrinogen-like domain lectins, the galectins and calnexin/calreticulin (Kilpatrick, 2002; Wang and Wang, 2013; Tassanakajon et al., 2013). The members of lectins exert their functions via mainly the carbohydrate recognition domain (CRD) and have various functions in shrimp innate immunity, including phagocytosis, melanization, respiratory burst, agglutination, and antibacterial and antiviral responses (Wang and Wang, 2013). C-type lectins (CTLs), a large subgroup of lectins extensively found in penaeid shrimps, have received the most attention and have been reported in many studies (Wang et al., 2009a; Zhao et al., 2009; Ma et al., 2009; Song et al., 2010; Li et al., 2014; Thepnarong et al., 2015; Wongpanya et al., 2017). Investigating novel CTLs in shrimp is important for enriching our understanding of the innate immune system of invertebrates and proposing effective strategies to protect shrimp against pathogen infections.

In this study, two novel CTLs were identified from the kuruma shrimp *Marsupenaeus japonicus*, and their tissue distributions and transcriptional profiles in response to WSSV and *V. parahaemolyticus* challenges were elucidated. Moreover, a glutathione-S-transferase (GST) pull-down assay was employed to investigate the interactions between the two novel CTLs and four WSSV envelope proteins, and the antibacterial and binding activities of the two CTLs against *V. parahaemolyticus* were analyzed. The present findings allow us to gain new insights into the multiple functions of CTLs in shrimp innate immunity and provide promising candidate agents to control and cure the diseases caused by WSSV and *V. parahaemolyticus*.

2. Materials and methods

2.1. Ethics statement

M. japonicus is not an endangered or protected species, and there is no requirement for ethical approval to perform experiments involving this species in China.

2.2. Animals

All *M. japonicus* prawns (11.40 g ± 1.39 g body weight) were collected from an aquaculture farm in Dongshang (Zhangzhou, Fujian, China) and were acclimated in environmentally controlled rectangular tanks (70 cm × 45 cm × 20 cm) with aerated seawater at a salinity of 28‰ before experimentation. The seawater was renewed daily, and the prawns were fed twice daily with commercial pellets.

2.3. Cloning of full-length cDNA sequences of MjCTL3 and MjCTL4

Total RNA was extracted using RNAiso Plus (Takara, Japan) following the manufacturer's instructions. The full-length cDNA sequences of MjCTL3 and MjCTL4 were obtained by reverse transcription PCR and RACE methods using a SMARTer™ RACE cDNA Amplifcation Kit (Takara, Japan) according to the manufacturer's protocols. The primers used for PCRs are listed in Table 1. The amplification products were ligated into the pMD19-T vector (Takara, Japan) and sequenced in both directions. The sequences were identified using the BLAST program (http://www.ncbi.nlm.gov/blast).

2.4. Bioinformatics analysis

The open reading frames (ORFs) of the MjCTL3 and MjCTL4 cDNA sequences were predicted using ORF Finder (http://www.ncbi.nlm.nih.gov/gorf/gorf.html) and the corresponding amino acid (aa) sequences were deduced by DNAMAN software. Protein molecular masses and the

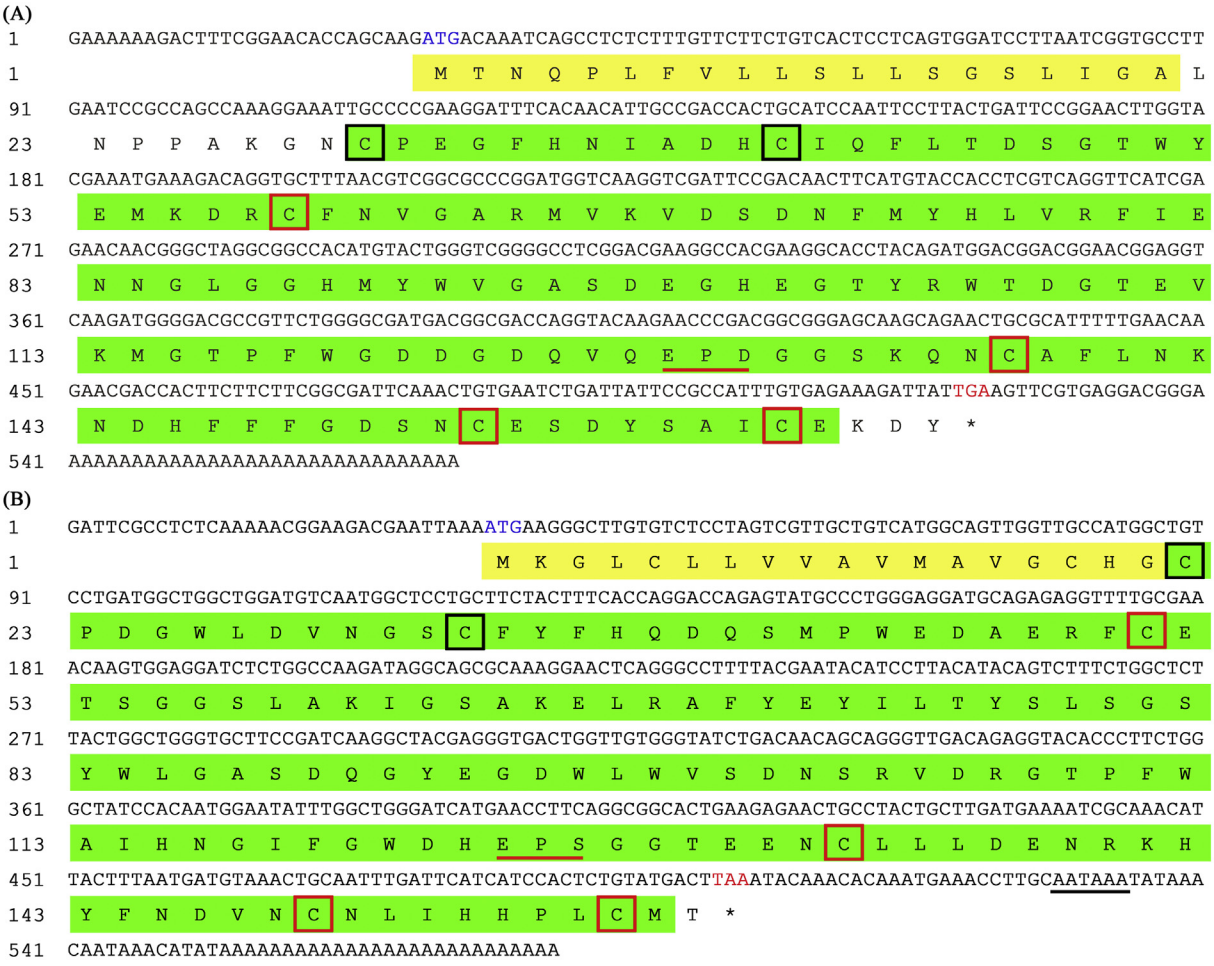

Fig. 1. Complete nucleotide and deduced aa sequences of MjCTL3 (A) and MjCTL4 (B) cDNA in *M. japonicus*.
Blue letters indicate the start sites, and red letters represent the stop codons. The signal peptide is shaded in yellow and the CRD is highlighted in green. Four highly conserved cysteine residues for establishing two internal disulfide bonds are shown by red boxes, and two additional cysteine residues located at the N-terminus are shown by black boxes. The mannose-binding motif is underlined in red, and the polyadenylation signal is underlined in black. (For interpretation of the references to colour in this figure legend, the reader is referred to the web version of this article.)

isoelectric points (pIs) were predicted using the ProtParam program (http://web.expasy.org/protparam/). Signal peptides were predicted by the SignalP 5.0 server (http://www.cbs.dtu.dk/services/SignalP/). Transmembrane domains were predicted by HMMTOP 2.0 (http://www.enzim.hu/hmmtop/html/submit.html). Identities of deduced amino acid (aa) sequences were determined using BioEdit (http://www.mbio.ncsu.edu/BioEdit/bioedit.html). Functional domains were predicted by SMART (http://smart.embl-heidelberg.de/). Multiple alignments were performed using ClustalW and the multiple alignment display program ESPript3.0 (http://espript.ibcp.fr/ESPript/ESPript/). A neighbor-joining phylogenetic tree was constructed by MEGA 5.05 with 1000 bootstrap replicates.

2.5. Tissue expression analysis of MjCTL3 and MjCTL4

The expression profiles of MjCTL3 and MjCTL4 in various tissues (hepatopancreas, gill, hemocytes, muscle, heart, stomach, intestine and eyestalk) from six prawns were individually tested with three technical replicates by quantitative real-time RT-PCR (qRT-PCR). qRT-PCR was performed on an Applied Biosystems QuantStudio 6 Flex Real-time PCR System (Applied Biosystems, USA) using SYBR® Premix ExTaq II (2×) (Takara, Japan) according to the manufacturer's protocols. *M. japonicus* elongation factor 1-α (EF1-α) served as the reference for internal standardization. The specific primers for qRT-PCR are listed in Table 1. Melting curve analysis was performed at the end of the reaction to confirm that only one PCR product was amplified and detected. The relative gene expression level was calculated using the $2^{-\Delta\Delta Ct}$ method (Livak and Schmittgen, 2001). All data were presented as the mean ± standard deviation (SD) and analyzed by one-way analysis of variance (ANOVA) using SPSS 17.0 software. *P*-values < .05 were considered statistically significant.

2.6. Expression alterations of the two CTLs in M. japonicus challenged by WSSV and V. parahaemolyticus

In the immune challenge experiment, shrimp were intramuscularly injected with 50 μL of saline (0.9% NaCl) containing WSSV (2×10^6 virions/mL) or *V. parahemolyticus* (2×10^5 CFU/mL). Meanwhile, shrimp injected with saline served as controls. At 3 h, 6 h, 12 h, 24 h, 48 h, 72 h and 96 h post injection (hpi), the hepatopancreas was dissected from six randomly sampled shrimp from each group. All samples were immediately frozen at −80 °C until the extraction of total RNA for analysis. The expression patterns of the two CTLs in the hepatopancreas of *M. japonicus* challenged by WSSV and *V. parahaemolyticus* were analyzed by qRT-PCR as described above.

2.7. Expression of recombinant proteins

cDNA fragments encoding the VP19, VP24, VP26 and VP28 peptides were amplified using primers with the restriction sites BamH I and EcoR

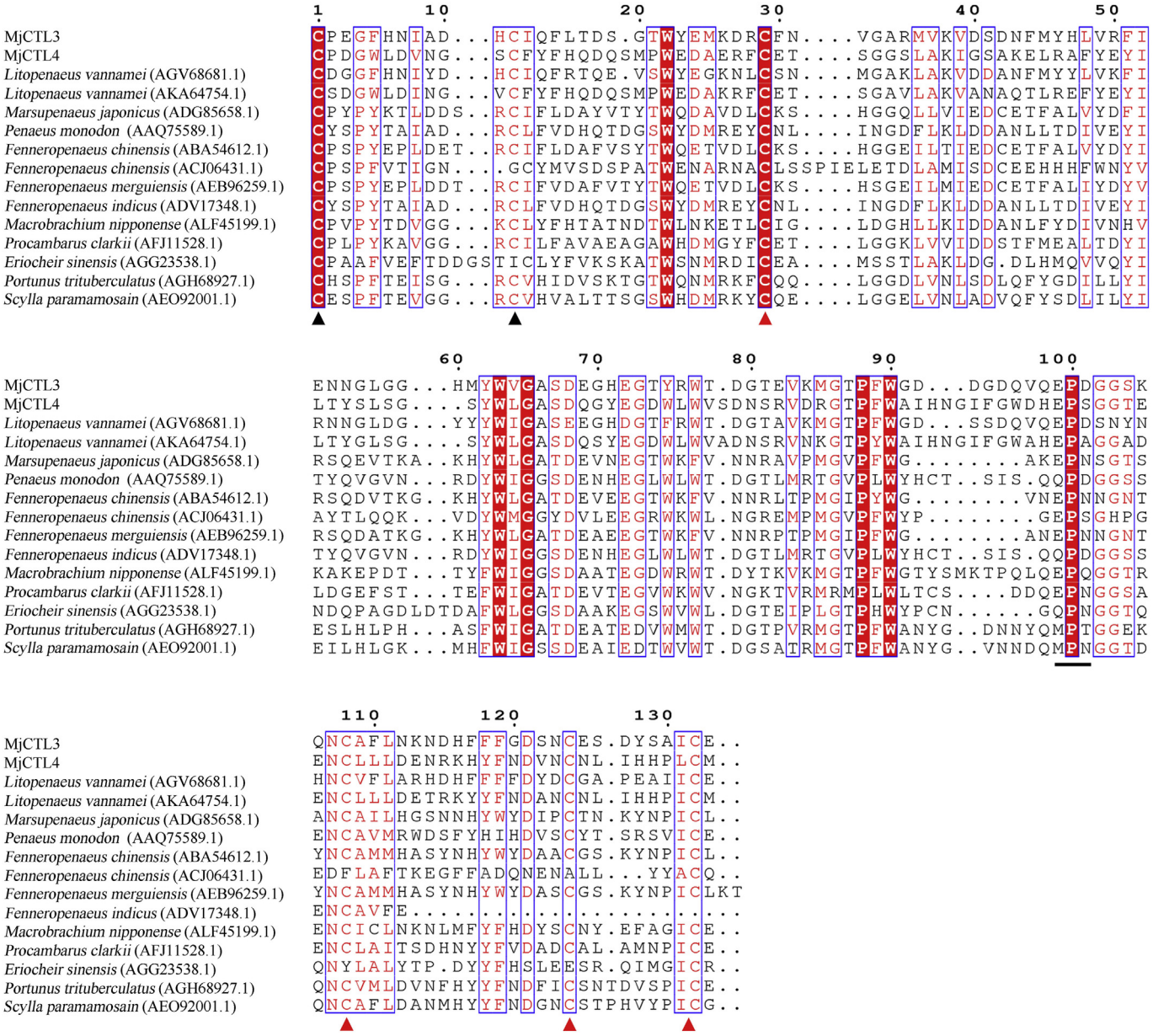

Fig. 2. Multiple alignments of the CRDs of MjCTL3 and MjCTL4 with other known CTL sequences.
Highly conserved aa residues are shown by blue boxes, and identical residues are shaded in red. Four highly conserved cysteine residues for establishing two internal disulfide bonds are marked with red triangles and two additional cysteine residues located at the N-terminus are marked with black triangles. The mannose-binding motif is underlined in black. (For interpretation of the references to colour in this figure legend, the reader is referred to the web version of this article.)

I (Table 1). The target cDNA fragment was ligated into the expression vector pGEX-4 T-1 with a GST tag. The cDNA fragments encoding the CRDs of the two CTLs were amplified using primers with the restriction sites EcoR I and Hind III (Table 1) and ligated into a pET-32a expression vector with a hexahistidine tag. Recombinant plasmids confirmed by sequencing were transformed into *Escherichia coli* BL21 (DE3) pLysS Chemically Competent Cells (TransGen Biotech, China) and induced at 18 °C for 12 h with isopropyl-β-thiogalactopyranoside (IPTG) at a final concentration of 0.1 mM. The induced bacterial pellets were collected by centrifugation (10,000 ×*g*) for 10 min at 4 °C and then suspended in 1 × PBS and lysed. The supernatants were collected by centrifugation (10,000 ×*g*) for 30 min at 4 °C. The recombinant proteins, namely, GST-VP19, GST-VP24, GST-VP26, GST-VP28, His-CRD3 and His-CRD4, in the supernatants were ascertained by sodium dodecyl sulfate-polyacrylamide gel electrophoresis (SDS-PAGE) and western blot analysis. Western blot was performed using an anti-GST/anti-His mouse monoclonal antibody (mAb) (TransGen Biotech, China) as primary antibody, and a HRP-linked goat anti-mouse antibody (TransGen Biotech, China) served as the secondary antibody.

2.8. GST pull-down assay

The GST pull-down assay was performed as previously described with slight modification. The lysate supernatants of induced bacteria that expressed GST-VP19, GST-VP24, GST-VP26, GST-VP28 and the negative control protein GST were incubated with glutathione-coupled Sepharose beads (TransGen Biotech, China) for 2 h at 4 °C with gentle rocking motion. Then, the beads were washed 7 times with 1 mL of wash solution (1 × PBS and 1‰ Triton X-100) to remove unbound proteins. The lysate supernatants of induced bacteria that expressed His-CRD3, His-CRD4 and the negative control protein rTrx-His were incubated with the beads coupled with GST-VP19, GST-VP24, GST-

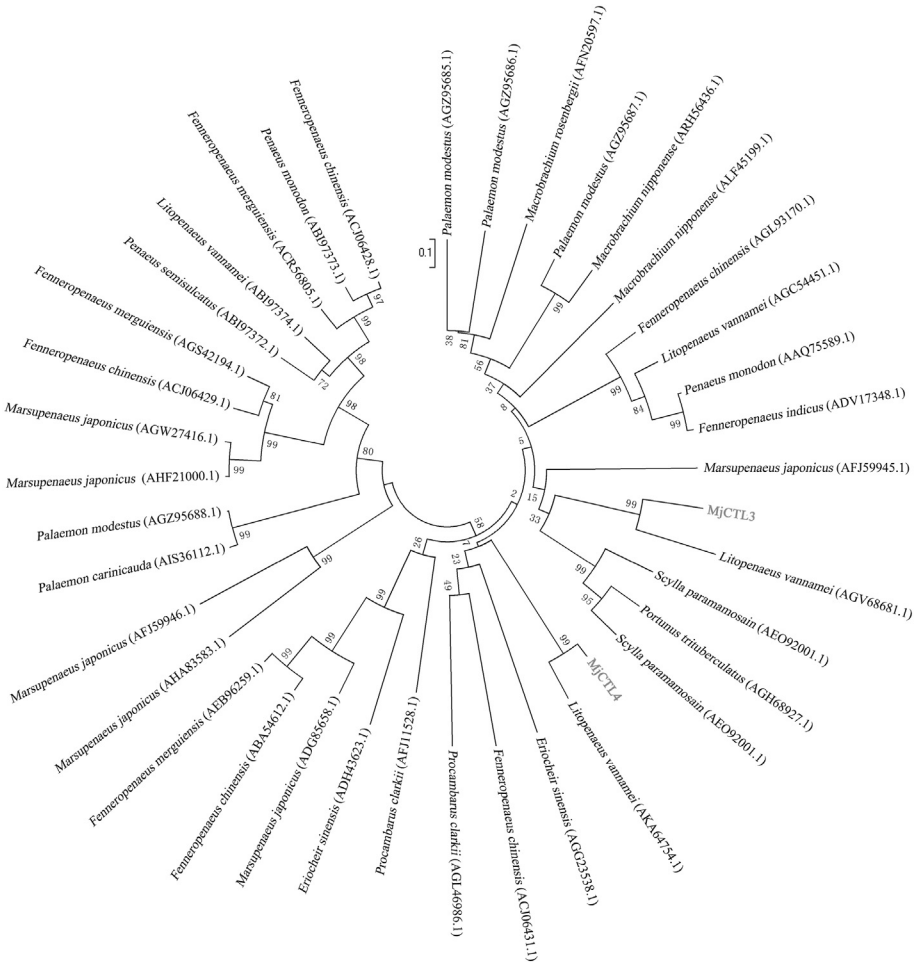

Fig. 3. Phylogenetic analysis of MjCTL3 and MjCTL4.
The tree topology was constructed by the neighbor-joining method and evaluated by 1000 replication bootstraps with MEGA 5.0 based on the deduced aa sequence alignments with ClustalW. The numbers at the forks indicate the bootstrap proportions. The two CTLs obtained in this study are shown in red. (For interpretation of the references to colour in this figure legend, the reader is referred to the web version of this article.)

VP26, GST-VP28 and GST at 4 °C for 4 h with gentle rotation. After that, the beads were washed 7 times with 1 mL of wash solution, re-suspended in 2 × SDS-PAGE loading buffer (Sangon Biotech, China) and analyzed by SDS-PAGE and western blot as described above.

2.9. Purification of recombinant proteins

The purification of His-CRD3, His-CRD4 and rTrx-His was performed on an AKTA Purifier 100 System (GE Healthcare, USA) using affinity chromatography with a HisTrap™ FF crude column (GE Healthcare, USA) according to the manufacturer's instructions. The bacterial pellets that expressed the recombinant proteins were collected and resuspended in Tris-HCl buffer (50 mM Tris-HCl, 500 mM NaCl, 20 mM imidazole, pH 7.8). The cells were lysed and the supernatants were collected as described above. Then, the supernatants were filtered through a 0.22 μm membrane and injected into the HisTrap™ FF crude column via siphon. The bound protein was eluted with a gradient elution buffer (50 mM Tris-HCl, 500 mM NaCl, 20/50/100/200/300/500 mM imidazole, pH 7.8), and the eluent was collected and analyzed by SDS-PAGE and Coomassie Blue staining to examine the purity of the target proteins. Finally, the target protein fractions were desalted by dialyzing against Tris-HCl buffer (50 mM Tris-HCl, 50 mM NaCl, pH 7.8) followed by ultra-pure water. The target proteins were collected and stored at −80 °C, and the protein concentrations were measured using BCA protein assay kits (Solarbio, China).

2.10. Anti-V. parahaemolyticus activity assay of the recombinant proteins

V. parahaemolyticus suspended in TBS (50 mM Tris-HCl, 50 mM NaCl, pH 7.5) or TBS−Ca^{2+} (50 mM Tris-HCl, 50 mM NaCl, 10 mM $CaCl_2$, pH 7.5) at a concentration of 2.6×10^7 CFU/mL was used for the antibacterial activity test. Fifty microliters of recombinant proteins (250 μg/mL) were mixed with the same volume of *V. parahaemolyticus* solution and incubated at 28 °C for 2 h. Then, the mixtures were diluted (10^4-fold) and spread on Mueller-Hinton agar plates, and the CFU were calculated after culturing for 16 h at 28 °C. Ultra-pure water and rTrx-His were used as a blank control and negative control, respectively, and each group was repeated three times.

2.11. Binding assay between the recombinant proteins and V. parahaemolyticus

To confirm the interaction between the two CRDs and *V. parahaemolyticus*, a binding assay was employed to determine the binding activity of the two CRDs against *V. parahaemolyticus*. Fifty microliters of recombinant proteins (250 μg/mL) were mixed with the same volume of *V. parahaemolyticus* solution (2.6×10^7 CFU/mL) and incubated at 28 °C for 2 h under slight rotation. The bacterial pellets were harvested by centrifugation at 5000 rpm for 10 min and washed five times with solution buffer. Bindings between recombinant proteins and *V. parahaemolyticus* was ascertained by SDS-PAGE and western blot analysis as described above.

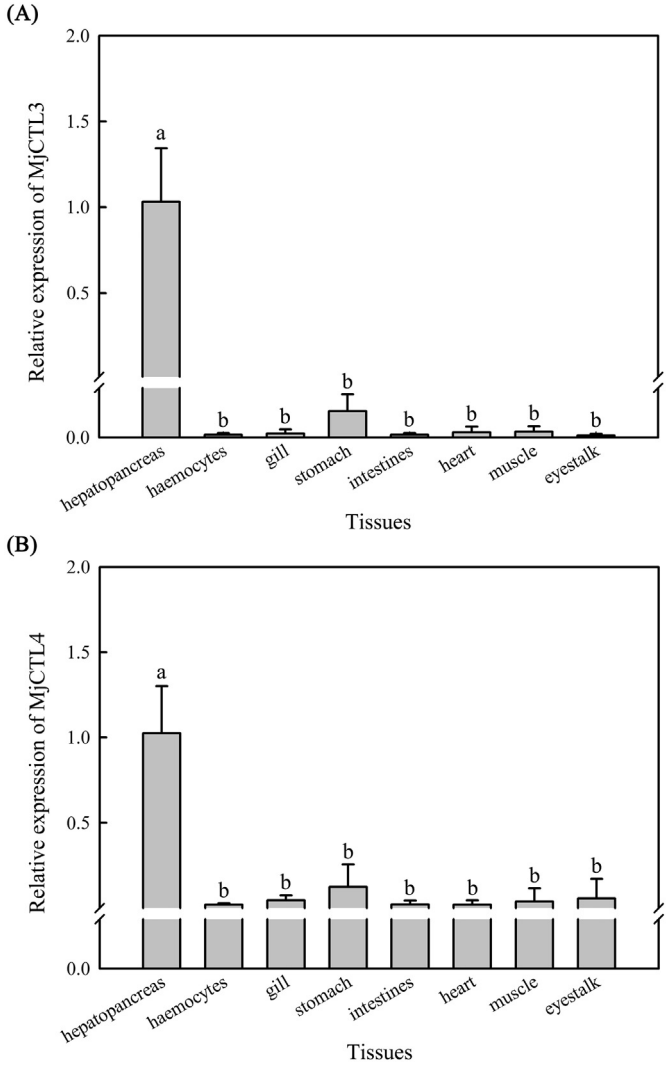

Fig. 4. Tissue distributions of MjCTL3 (A) and MjCTL4 (B) mRNA in *M. japonicus*.
Expression levels in hemocytes, gills, stomach, intestine, heart, muscle and eyestalk are normalized to those in the hepatopancreas. Each bar represents the mean ± SD (n = 6). A significant difference between groups at $p < .05$ (n = 6, ANOVA) is indicated by different letters above the bars.

3. Results

3.1. Sequence analysis of the two CTLs

The full-length cDNA of MjCTL3 (GenBank accession number: MN183127) was 571 bp long with an ORF of 495 bp. The ORF encoded a polypeptide of 164 aa, which had a predicted molecular weight of 18.35 kDa and a theoretical pI of 4.59. The full-length cDNA of MjCTL4 (GenBank accession number: MN183128) spanned 579 bp and comprised an ORF of 471 bp encoding a polypeptide of 156 aa. The predicted molecular weight of MjCTL4 was 17.58 kDa and the theoretical pI was 4.73. The deduced aa sequences of MjCTL3 and MjCTL3 exhibited the typical features of CTLs, including a signal peptide in the N-terminus and a single CRD with a characteristic mannose-binding motif (an EPD motif in CRD3 and an EPS in CRD4) in the mature peptide (Fig. 1). The CRD in both MjCTL3 and MjCTL4 possessed four cysteine residues (Cys57, Cys136, Cys152 and Cys160 in MjCTL3; Cys48, Cys130, Cys146 and Cys154 in MjCTL4) that were essential for the formation of two internal disulfide bonds to stabilize the CRD structure, and two additional disulfide-bonded cysteine residues were located at the N-terminus (Cys29 and Cys40 in MjCTL3; Cys19 and Cys30 in MjCTL4) (Fig. 1). Additionally, a transmembrane domain (L^6-N^{22}) was predicted in the N-terminus of the deduced MjCTL3 protein.

Homology comparisons showed that the deduced aa sequences of MjCTL3 and MjCTL4 had high identity to CTL3 (AGV68681.1, 57.5%) and CTL4 (AKA64754.1, 81.4%) in *Litopenaeus vannamei*, respectively, and showed 28.9% identity with each other. Multiple sequence alignments showed that the six cysteine residues found in the CRD of CTLs are well conserved among various crustaceans, and the mannose-binding motif EP* exhibited mutations in different crustaceans (Fig. 2). Phylogenetic analysis showed that MjCTL3 and MjCTL4 were most closely phylogenetically related to CTL3 (AGV68681.1) and CTL4 (AGV68681.1) identified from L. *vannamei* (Fig. 3).

3.2. Tissue distribution of the two CTLs

Tissue distribution analysis showed that MjCTL3 and MjCTL4 were both predominantly expressed in the hepatopancreas and weakly expressed in other tested tissues, including gills, hemocytes, muscle, heart, stomach, intestine and eyestalk (Fig. 4).

3.3. Expression profiles of the two CTLs in M. japonicus challenged with WSSV and V. parahaemolyticus

Significant increases in MjCTL3 and MjCTL4 expression were observed in the hepatopancreas of *M. japonicus* challenged with WSSV and *V. parahaemolyticus* (Fig. 5). The transcriptional level of MjCTL3 in the hepatopancreas of shrimp challenged with WSSV was up-regulated 6.01-fold at 12 hpi (Fig. 5A). The expression level of MjCTL3 in the hepatopancreas of shrimp challenged with *V. parahaemolyticus* started to increase by 1.98-fold at 6 hpi and reached a maximum level at 24 hpi, with a 6.66-fold increase (Fig. 5A). The transcription of MjCTL3 in shrimp challenged with WSSV or *V. parahaemolyticus* was down-regulated at both 48 hpi and 72 hpi (Fig. 5A) and then recovered to a basal level at 96 hpi. The expression level of MjCTL4 in the hepatopancreas of shrimp challenged with WSSV and *V. parahaemolyticus* was elevated at 96 hpi, with 1.56-fold and 1.92-fold increases, respectively (Fig. 5B).

3.4. Protein interaction analysis between the two CTLs and WSSV envelope proteins

To investigate the interaction between WSSV envelope proteins and the two CTLs, recombinant proteins, namely, GST, GST-VP19, GST-VP24, GST-VP26, GST-VP28, His-CRD3 and His-CRD4, were produced in an *E. coli* expression system. SDS-PAGE and western blot analysis showed that the recombinant proteins exhibited the expected size (Fig. 6). Interactions between the four WSSV envelope proteins and the two CTLs were identified by GST pull-down assay. The results showed that His-CRD3 and His-CRD4 were bound to the four WSSV envelope proteins with a GST-tag but not to the GST protein alone (Fig. 7). As a control, rTrx-His did not bind to GST or GST fused envelope proteins. Taken together, these results indicated that there was an interaction between the two CTLs and the four WSSV envelope proteins.

3.5. The antibacterial and binding activities of the two CTLs against V. parahaemolyticus

To investigate the biological activities of the two CTLs toward *V. parahaemolyticus*, affinity chromatography was carried out to purify the recombinant proteins. SDS-PAGE showed that a single target band was detected in the eluent that eluted with elution buffer containing 100 mM imidazole (Fig. 8), indicating that there was no contamination of the purified recombinant proteins. The ant-*V. parahaemolyticus* assay showed that both recombinant proteins exhibited antibacterial activity against *V. parahaemolyticus* and that His-CRD3 showed a greater anti-*V. parahaemolyticus* capacity than His-CRD4 (Fig. 9). In the TBS buffer, the

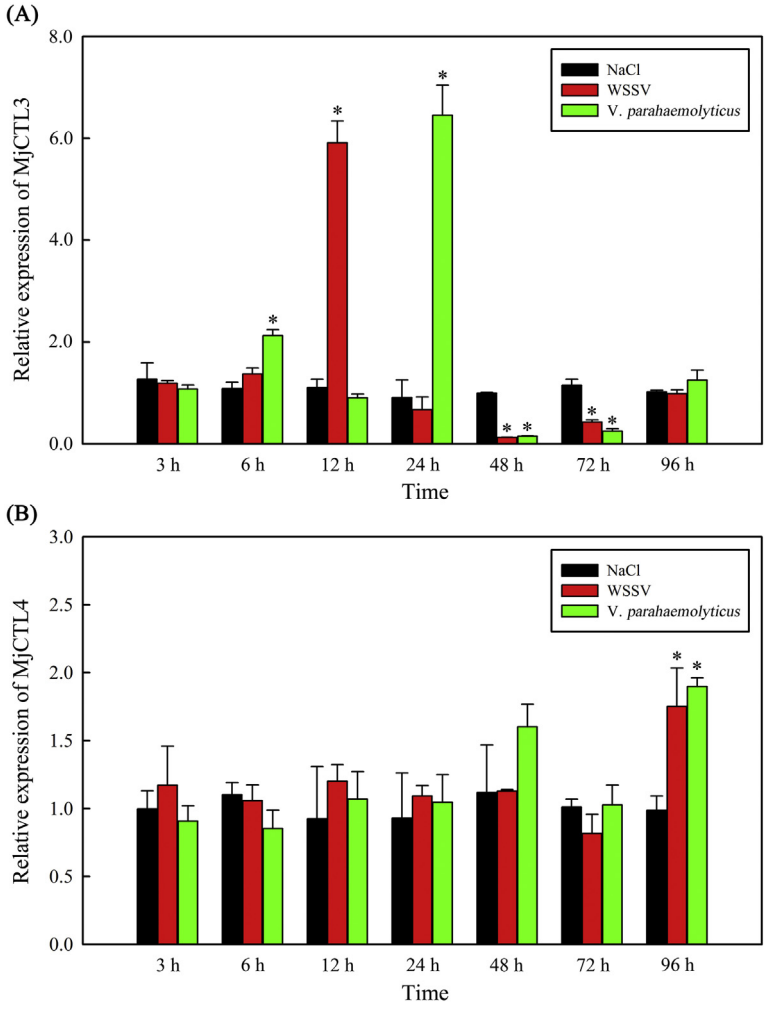

Fig. 5. Expression profiles of MjCTL3 (A) and MjCTL4 (B) in the hepatopancreas of *M. japonicus* challenged with WSSV and *V. parahaemolyticus*. Each bar represents the mean ± SD (n = 6). A significant difference between the control group and pathogen infection groups at $p < .05$ (n = 6, ANOVA) is indicated by an * above the bars.

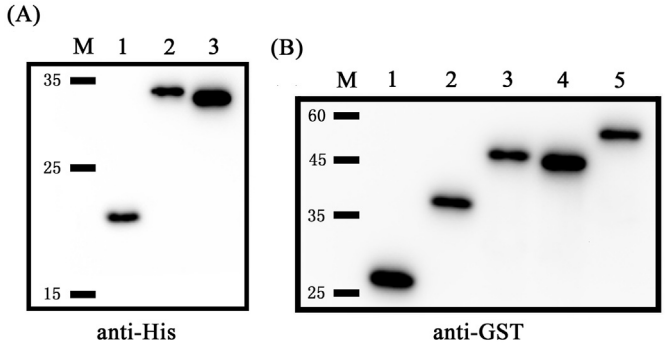

Fig. 6. Western blot analysis of the recombinant proteins.
A: Western blot analysis of His-CRD3 and His-CRD4. M: protein molecular standard (kDa); lane 1: rTrx-His; lane 2: His-CRD3; lane 3: His-CRD4. B: Western blot analysis of GST-VP19, GST-VP24, GST-VP26 and GST-VP28. M: protein molecular standard (kDa); lane 1: GST; lane 2: GST-VP19; lane 3: GST-VP24; lane 4: GST-VP26; lane 5: GST-VP28. anti-His and anti-GST indicated proteins tested by western blot with anti-His mAb and anti-GST mAb, respectively.

CFU of *V. parahaemolyticus* that was treated with His-CRD3 and His-CRD4 significantly decreased 40.26-fold and 2.60-fold, respectively, compared to that in the blank control group. In the TBS−Ca^{2+} buffer, the CFU of *V. parahaemolyticus* that was treated with His-CRD3 and His-CRD4 significantly decreased 21.84-fold and 3.96-fold, respectively, compared to that in the blank control group. Western blot analysis revealed that both of the recombinant proteins exhibited a binding capability toward *V. parahaemolyticus* (Fig. 10).

4. Discussion

CTLs are crucial components in the innate immune system of shrimp. To date, a substantial number of CTLs involved in host defense against bacterial and viral infection have been identified and characterized in shrimps, such as L. *vannamei* (Ma et al., 2007; Zhao et al., 2009; Zhang et al., 2009a; Wei et al., 2012; Li et al., 2014), *Penaeus monodon* (Ma et al., 2008; Wongpanya et al., 2017), *M. japonicus* (Song et al., 2010; Xu et al., 2014), *Fenneropenaeus chinensis* (Sun et al., 2008; Wang et al., 2009a; Wang et al., 2009b; Zhang et al., 2009b; Xu et al., 2010) and *F. merguiensis* (Rattanaporn and Utarabhand, 2011; Thepnarong et al., 2015; Runsaeng et al., 2015; Kwankaew et al., 2018). Herein, two novel CTLs from *M. japonicus* were characterized and functionally analyzed. The two CTLs were distinguished from previously identified CTLs in *M. japonicus* and shared the highest homology and closest phylogenetic relationship to CTL3 (AGV68681.1, 57.5%) and CTL4 (AKA64754.1, 81.4%) identified from L. *vannamei*, respectively. Generally, CTLs contain one or two CRDs with the characteristic mannose-binding motif EPN or galactose-binding motif QPD, however, mutations of the EPN and QPD motif, such as EPD, EPS, EPA,

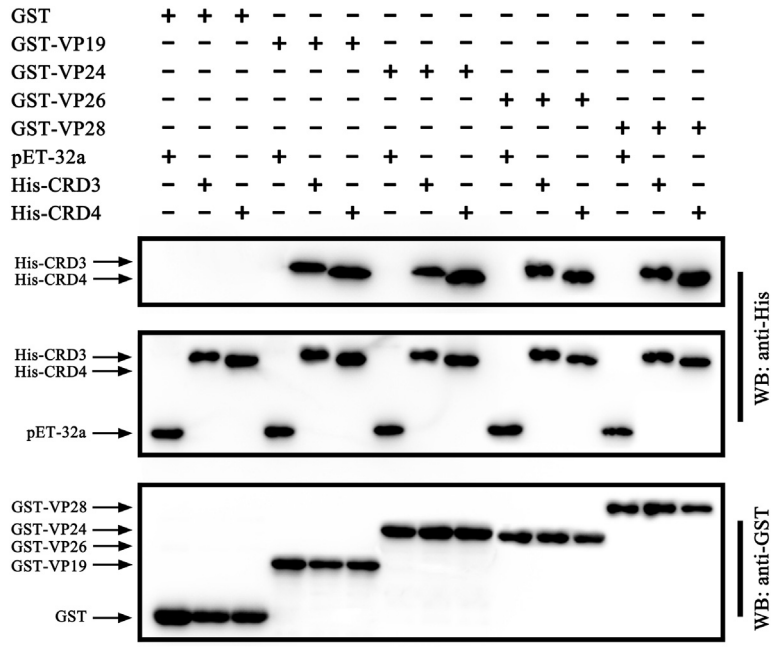

Fig. 7. GST pull-down assay between the two CRDs and four WSSV envelope proteins.
WB: anti-His and WB: anti-GST indicate proteins tested by western blot with an anti-His mAb and anti-GST mAb, respectively. + indicates the proteins used in the GST pull-down assay.

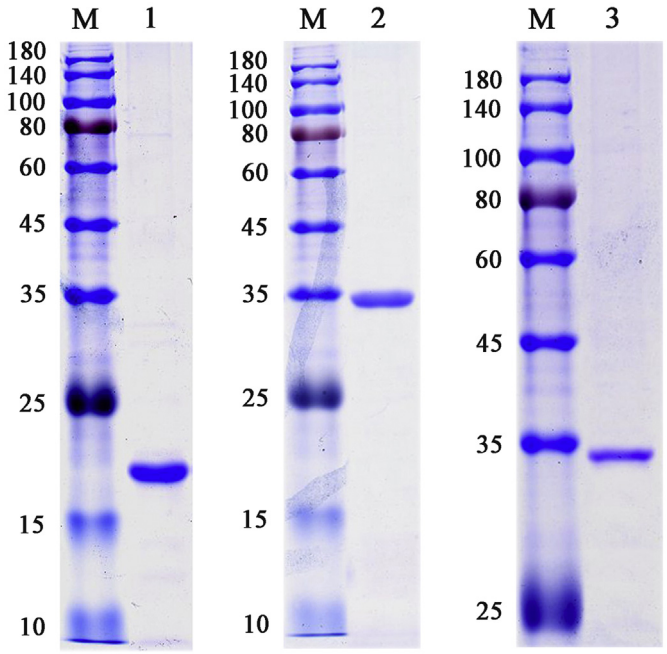

Fig. 8. SDS-PAGE analyses of purified recombinant proteins.
M: protein molecular standard (kDa); lane 1: rTrx-His; lane 2: His-CRD3; lane 3: His-CRD4.

EPQ and QPN, have been found in CTLs identified from different species (Wang and Wang, 2013). In this study, the two novel CTLs identified from *M. japonicus* both contained a single CRD with a characteristic EP* motif that is indicative of mannose-binding specificity. The two CTLs were predicted to be secreted proteins due to the existence of a signal peptide, implying that the two CTLs might be secreted as defense molecules. Interestingly, a transmembrane domain was also found in the N-terminus of MjCTL3, indicating that MjCTL3 might be a transmembrane protein and function as a membrane receptor to recognize invading pathogens.

The tissue distribution of CTLs in shrimp was shown to be variable across species.

Numerous CTLs in shrimp are expressed in mainly or solely the hepatopancreas (Ma et al., 2008; Sun et al., 2008; Wang et al., 2009a; Zhao et al., 2009; Zhang et al., 2009b; Thepnarong et al., 2015), and some CTLs are predominantly expressed in hemocytes, gills or brains (Liu et al., 2007; Zhang et al., 2009a; Li et al., 2014; Kwankaew et al., 2018). In addition, CTLs are also expressed in the stomach, intestine, epithelium, muscle and eyestalk of shrimp (Zhang et al., 2009b; Li et al., 2014). In this study, the two CTLs could be ubiquitously detected in all examined tissues with the highest expression level in the hepatopancreas, which is consistent with the fact that the hepatopancreas is the main tissue that synthesizes shrimp lectins. In addition to acting as a master organ in digestion and metabolism, the hepatopancreas is an important immune organ of crustaceans as well (Rőszer, 2014). The high expression of the two CTLs in the hepatopancreas might indicate their important role in the immune response.

As multifunctional immune molecules in shrimp, CTLs can respond to various pathogens, such as *V. parahaemolyticus*, *V. harveyi*, *V. anguillarum* and WSSV (Zhang et al., 2009b; Li et al., 2014; Thepnarong et al., 2015). In the current study, challenging *M. japonicus* with WSSV and *V. parahaemolyticus* induced the transcription of MjCTL3 in the hepatopancreas to obtain peaks at 12 hpi and 24 hpi, respectively. Meanwhile, the transcriptional levels of MjCTL4 reached a maximum at 96 h post challenge with the two pathogens. The significant increases in the two CTLs in response to WSSV and *V. parahaemolyticus* infection implied their potential function in defense against the two pathogens. Although transcription of the two CTLs was dramatically increased in shrimp infected with the two pathogens, quite different expression patterns were observed. MjCTL3 responded more quickly and dramatically to the two pathogens than MjCTL4, suggesting that the former may play a more dominant role in resisting the two pathogens. It is notable that the transcription level of MjCTL3 in the hepatopancreas significantly dropped at 48 h and 72 h post challenge with WSSV and *V. parahaemolyticus*. A CTL in the liver of *Larimichthys crocea* displayed an expression pattern similar to that of MjCTL3 in response to WSSV infection (Lv et al., 2016), however, the expression level of a CTL in the hepatopancreas of L. *vannamei* initially decreased and then increased in

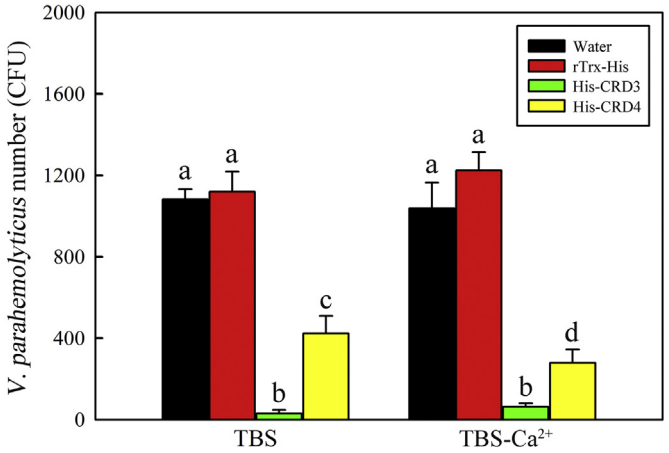

Fig. 9. Anti-*V. parahaemolyticus* activity of recombinant proteins.
Each bar represents the mean ± SD ($n = 3$). A significant difference between groups at $p < .05$ (n = 3, ANOVA) is indicated by different letters above the bars.

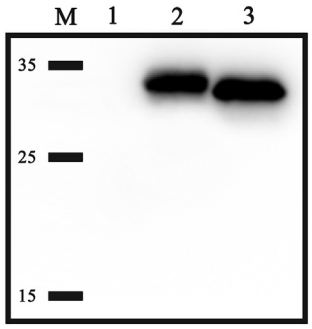

Fig. 10. *V. parahaemolyticus* binding activity of recombinant proteins.
M: protein molecular standard (kDa); lane 1: rTrx-His; lane 2: His-CRD3; lane 3: His-CRD4.

WSSV-challenged shrimp (Ma et al., 2007). These findings implied that the hosts may employ different ways to defend against pathogen infection.

The primary function of CTLs is serving as PRRs that recognize and bind to the PAMPs on the surface of microbes. To further ascertain the roles of the two CTLs in WSSV and *V. parahaemolyticus* infection, recombinant proteins of the CRDs of the two CTLs (His-CRD3 and His-CRD4) and four WSSV envelope proteins (GST-VP19, GST-VP24, GST-VP26, and GST-VP28) were successfully produced, and the interactions between the two CRDs and the four envelope proteins were analyzed by GST pull-down assays. VP19, VP24, VP26 and VP28 are four major envelope proteins of WSSV and have been shown to be involved in the virus infection of shrimp (Yi et al., 2004; van Hulten et al., 2001; Xie and Yang, 2006; Zhou et al., 2009; Li et al., 2016). Herein, the results presented by the GST pull-down assay showed that the two CRDs both directly interacted with the four WSSV envelope proteins. Furthermore, bacterial binding activity analysis showed that both of the CRDs possessed binding ability to *V. parahaemolyticus*. These data indicated that the two CTLs may act as PRRs to recognize WSSV and *V. parahaemolyticus* by binding to the pathogens. Moreover, the direct interaction between the two CTLs and WSSV envelope proteins might attenuate WSSV infectivity and impede virus entry into the cells (Xiao et al., 2018).

In addition to serving as PRRs, CTLs also work to eliminate invading pathogens by directly agglutinating or killing microorganisms. Numerous CTLs have been shown to exhibit their antibacterial activity in a Ca^{2+}-dependent manner (Li et al., 2014; Li et al., 2015; Lv et al., 2016), however, some CTLs were demonstrated to be Ca^{2+}-independent (Song et al., 2010). In this study, the antibacterial assay showed that the two CTLs possessed antibacterial activity against *V. parahaemolyticus* in either the presence or absence of Ca^{2+}. MjCTL3 displayed stronger antibacterial activity against *V. parahaemolyticus* than MjCTL4, together with the fact that the expression of MjCTL3 increased more quickly and strongly than MjCTL4 expression in shrimp challenged with *V. parahaemolyticus*, it was reasonable to infer that MjCTL3 might play a more crucial role in immune defense against *V. parahaemolyticus* invasion. Interestingly, the anti-*V. parahaemolyticus* activity of MjCTL4 was obviously promoted in the presence of Ca^{2+}. Similar results have been reported for other CTLs identified from *M. japonicus*, and the mutation of the calcium binding motif might contribute to the Ca^{2+}-independent activity of MjCTLs (Song et al., 2010).

5. Conclusion

In the present study, two novel CTLs were identified and characterized from *M. japonicus*. The two CTLs both contained a single CRD and were predominately expressed in the hepatopancreas. The transcription of the two CTLs was enhanced by WSSV and *V. parahaemolyticus* infection, and MjCTL3 exhibited a higher up-regulation level than MjCTL4. GST pull-down assays showed that there was a direct interaction between the two CTLs and WSSV envelope proteins. Additionally, the two CTLs also displayed antibacterial and binding activities to *V. parahaemolyticus*, indicating that the two CTLs were involved in the recognition and elimination of *V. parahaemolyticus*. The multiple immune functions exhibited by the two CTLs implied their promising application prospects in the control of disease caused by WSSV and *V. parahaemolyticus*.

Declaration of Competing Interest

The authors declare that they have no conflict of interest.

Acknowledgments

This research was supported by the Project of China Agriculture Research System (grant No. CARS-48), the Research Start-up Fund and the K. C. Wong Magna Fund of Ningbo University.

References

Cabello, F.C., Godfrey, H.P., Buschmann, A.H., Dölz, H.J., 2016. Aquaculture as yet another environmental gateway to the development and globalisation of antimicrobial resistance. Lancet Infect. Dis. 16, e127–e133.
Dam, T.K., Brewer, C.F., 2009. Lectins as pattern recognition molecules: the effects of epitope density in innate immunity. Glycobiol. 20, 270–279.
Flegel, T.W., 2012. Historic emergence, impact and current status of shrimp pathogens in Asia. J. Invertebr. Pathol. 110, 166–173.
Food and Agriculture Organization of the United Nations Global Production Statistics, 2019. http://www.fao.org/fishery/statistics/global-aquaculture-production/query/en (accessed 11 July 2019).
Holmström, K., Gräslund, S., Wahlström, A., Poungshompoo, S., Bengtsson, B.E., Kautsky, N., 2003. Antibiotic use in shrimp farming and implications for environmental impacts and human health. Int. J. Food Sci. Technol. 38, 255–266.
van Hulten, M.C.W., Witteveldt, J., Snippe, M., Vlak, J.M., 2001. White spot syndrome virus envelope protein VP28 is involved in the systemic infection of shrimp. Virol. 285, 228–233.
Joshi, J., Srisala, J., Truong, V.H., Chen, I.T., Nuangsaeng, B., Suthienkul, O., Lo, C.F., Flegel, T.W., Sritunyalucksana, K., Thitamadee, S., 2014. Variation in *Vibrio parahaemolyticus* isolates from a single Thai shrimp farm experiencing an outbreak of acute hepatopancreatic necrosis disease (AHPND). Aquac. 428, 297–302.
Karunasagar, I., Ababouch, L., 2012. Shrimp viral diseases, import risk assessment and international trade. Indian J. Virol. 23, 141–148.
Kennedy, J.F., Palva, P.M.G., Corella, M.T.S., Cavalcanti, M.S.M., Coelho, L.C.B.B., 1995. Lectins, versatile proteins of recognition: a review. Carbohydr. Polym. 26, 219–230.
Kilpatrick, D.C., 2002. Animal lectins: a historical introduction and overview. BBA-Gen. Subj. 1572, 187–197.
Kumar, B.K., Deekshit, V.K., Raj, J.R.M., Rai, P., Shivanagowda, B.M., Karunasagar, I., Karunasagar, I., 2014. Diversity of *Vibrio parahaemolyticus* associated with disease outbreak among cultured *Litopenaeus vannamei* (Pacific white shrimp) in India. Aquac. 433, 247–251.
Kwankaew, P., Praparatana, R., Runsaeng, P., Utarabhand, P., 2018. An alternative

function of C-type lectin comprising low-density lipoprotein receptor domain from *Fenneropenaeus merguiensis* to act as a binding receptor for viral protein and vitellogenin. Fish Shellfish Immunol. 74, 295–308.
Li, M., Li, C.Z., Ma, C.X., Li, H.Y., Zuo, H.L., Weng, S.P., Chen, X.H., Zeng, D.G., He, J.G., Xu, X.P., 2014. Identification of a C-type lectin with antiviral and antibacterial activity from pacific white shrimp *Litopenaeus vannamei*. Dev. Comp. Immunol. 46, 231–240.
Li, H., Zhang, H., Jiang, S., Wang, W.L., Xin, L.S., Wang, H., Wang, L.L., Song, L.S., 2015. A single-CRD C-type lectin from oyster *Crassostrea gigas* mediates immune recognition and pathogen elimination with a potential role in the activation of complement system. Fish Shellfish Immunol. 44, 566–575.
Li, Z.P., Li, F., Han, Y.L., Xu, L.M., Yang, F., 2016. VP24 is a chitin-binding protein involved in white spot syndrome virus infection. J. Virol. 90, 842–850.
Lightner, D.V., 2011. Virus diseases of farmed shrimp in the western hemisphere (the Americas): a review. J. Invertebr. Pathol. 106, 110–130.
Lightner, D.V., Redman, R.M., Pantoja, C.R., Tang, K.F.J., Noble, B.L., Schofield, P., Mohney, L.L., Nunan, L.M., Navarro, S.A., 2012. Historic emergence, impact and current status of shrimp pathogens in the Americas. J. Invertebr. Pathol. 110, 174–183.
Liu, Y.C., Li, F.H., Dong, B., Wang, B., Luan, W., Zhang, X.J., Zhang, L.S., Xiang, J.H., 2007. Molecular cloning, characterization and expression analysis of a putative C-type lectin (Fclectin) gene in Chinese shrimp *Fenneropenaeus chinensis*. Mol. Immunol. 44, 598–607.
Livak, K.J., Schmittgen, T.D., 2001. Analysis of relative gene expression data using real-time quantitative PCR and the $2^{-\Delta\Delta CT}$ method. Methods 25, 402–408.
Lv, C.H., Zhang, D.L., Wang, Z.Y., 2016. A novel C-type lectin, Nattectin-like protein, with a wide range of bacterial agglutination activity in large yellow croaker *Larimichthys crocea*. Fish Shellfish Immunol. 50, 231–241.
Ma, T.H.T., Tiu, S.H.K., He, J.G., Chan, S.M., 2007. Molecular cloning of a C-type lectin (LvLT) from the shrimp *Litopenaeus vannamei*: early gene down-regulation after WSSV infection. Fish Shellfish Immunol. 23, 430–437.
Ma, T.H.T., Benzie, J.A.H., He, J.G., Chan, S.M., 2008. PmLT, a C-type lectin specific to hepatopancreas is involved in the innate defense of the shrimp *Penaeus monodo*n. J. Invertebr. Pathol. 99, 332–341.
Manilal, A., Sujith, S., Selvin, J., Shakir, Chippu, Gandhimathi, R., Seghal Kiran, G., 2010. Virulence of vibrios isolated from diseased black tiger shrimp, *Penaeus monodon*, fabricius. J. World Aquacult. Soc. 41, 332–343.
Marques, M.R.F., Barracco, M.A., 2000. Lectins, as non-self-recognition factors, in crustaceans. Aquac. 191, 23–44.
Oakey, H.J., Smith, C.S., 2018. Complete genome sequence of a white spot syndrome virus associated with a disease incursion in Australia. Aquac. 484, 152–159.
Rattanaporn, O., Utarabhand, P., 2011. Molecular cloning of a C-type lectin with two CRD domains from the banana shrimp *Fenneropenaeus merguiensis*: early gene up-regulation after *Vibrio harveyi* infection. J. Invertebr. Pathol. 106, 196–204.
Rőszer, T., 2014. The invertebrate midintestinal gland ("hepatopancreas") is an evolutionary forerunner in the integration of immunity and metabolism. Cell Tissue Res. 358, 685–695.
Runsaeng, P., Thepnarong, S., Rattanaporn, O., Utarabhand, P., 2015. Cloning and the mRNA expression of a C-type lectin with one carbohydrate recognition domain from *Fenneropenaeus merguiensis* in response to pathogenic inoculation. Mol. Cell. Probes 29, 365–375.
Shinn, A.P., Pratoomyot, J., Griffiths, D., Trong, T.Q., VU, N.T., Jiravanichpaisal, P., Briggs, M., 2018. Asian shrimp production and the economic costs of disease. Asian Fish. Sci. 31, 29–58.
Song, K.K., Li, D.F., Zhang, M.C., Yang, H.J., Ruan, L.W., Xu, X., 2010. Cloning and characterization of three novel WSSV recognizing lectins from shrimp *Marsupenaeus japonicus*. Fish Shellfish Immunol. 28, 596–603.
Su, H.C., Liu, S., Hu, X.J., Xu, X.R., Xu, W.J., Xu, Y., Li, Z.J., Wen, G.L., Liu, Y.S., Cao, Y.C., 2017. Occurrence and temporal variation of antibiotic resistance genes (ARGs) in shrimp aquaculture: ARGs dissemination from farming source to reared organisms. Sci. Total Environ. 607, 357–366.
Sun, Y.D., Fu, L.D., Jia, Y.P., Du, X.J., Wang, Q., Wang, Y.H., Zhao, X.F., Yu, X.Q., Wang, J.X., 2008. A hepatopancreas-specific C-type lectin from the Chinese shrimp *Fenneropenaeus chinensis* exhibits antimicrobial activity. Mol. Immunol. 45, 348–361.
Tassanakajon, A., Somboonwiwat, K., Supungul, P., Tang, S., 2013. Discovery of immune molecules and their crucial functions in shrimp immunity. Fish Shellfish Immunol. 34, 954–967.
Thepnarong, S., Runsaeng, P., Rattanaporn, O., Utarabhand, P., 2015. Molecular cloning of a C-type lectin with one carbohydrate recognition domain from *Fenneropenaeus merguiensis* and its expression upon challenging by pathogenic bacterium or virus. J. Invertebr. Pathol. 125 (1–8).
Thitamadee. S., Prachumwat, A., Srisala, J., Jaroenlak, Pattana., Salachan, P. V., Sritunyalucksana, K., Flegel, T.W., Itsathitphaisarn, O., 2016. Review of current disease threats for cultivated penaeid shrimp in Asia. Aquac. 452, 69–87.
Thuy, H.T.T., Loan, T.T.C., 2011. Antibiotic contaminants in coastal wetlands from Vietnamese shrimp farming. Environ. Sci. Pollut. R. 18, 835–841.
Vazquez, L., Alpuche, J., Maldonado, G., Agundis, C., Pereyra-Morales, A., Zenteno, E., 2009. Immunity mechanisms in crustaceans. Innate Immun. 15, 179–188.
Verbruggen, B., Bickley, L., van Aerle, R., Bateman, K.S., Stentiford, G.D., Santos, E.M., Tyler, C.R., 2016. Molecular mechanisms of white spot syndrome virus infection and perspectives on treatments. Viruses 8, 23–51.
Vignesh, R., Karthikeyan, B.S., Periyasamy, N., Devanathan, K., 2011. Antibiotics in aquaculture: an overview. South Asian. J. Exp. Biol. 1, 114–120.
Wang, X.W., Wang, J.X., 2013. Diversity and multiple functions of lectins in shrimp immunity. Dev. Comp. Immunol. 39, 27–38.
Wang, X.W., Zhang, X.W., Xu, W.T., Zhao, X.F., Wang, J.X., 2009a. A novel C-type lectin (FcLec4) facilitates the clearance of *Vibrio anguillarum* in vivo in Chinese white shrimp. Dev. Comp. Immunol. 33, 1039–1047.
Wang, X.W., Xu, W.T., Zhang, X.W., Zhao, X.F., Yu, X.Q., Wang, J.X., 2009b. A C-type lectin is involved in the innate immune response of Chinese white shrimp. Fish Shellfish Immunol. 27, 556–562.
Wei, X.M., Liu, X.Q., Yang, J.M., Fang, J.H., Qiao, H.J., Zhang, Y., Yang, J.L., 2012. Two C-type lectins from shrimp *Litopenaeus vannamei* that might be involved in immune response against bacteria and virus. Fish Shellfish Immunol. 32, 132–140.
Wongpanya, R., Sengprasert, P., Amparyup, P., Tassanakajon, A., 2017. A novel C-type lectin in the black tiger shrimp Penaeus monodon functions as a pattern recognition receptor by binding and causing bacterial agglutination. Fish Shellfish Immunol. 60, 103–113.
Xiao, B., Fu, Q.H., Niu, S.W., Li, H.Y., Lv, K., Wang, S., Yin, Bin, Weng, S.P., Li, C.Z., He, J.G., 2018. Penaeidins are a novel family of antiviral effectors against WSSV in shrimp. BioRxiv 467571.
Xie, X.X., Yang, F., 2006. White spot syndrome virus VP24 interacts with VP28 and is involved in virus infection. J. Gen. Virol. 87, 1903–1908.
Xu, W.T., Wang, X.W., Zhang, X.W., Zhao, X.F., Yu, X.Q., Wang, J.X., 2010. A new C-type lectin (FcLec5) from the Chinese white shrimp *Fenneropenaeus chinensis*. Amino Acids 39, 1227–1239.
Xu, Y.H., Bi, W.J., Wang, X.W., Zhao, Y.R., Zhao, X.F., Wang, J.X., 2014. Two novel C-type lectins with a low-density lipoprotein receptor class a domain have antiviral function in the shrimp *Marsupenaeus japonicus*. Dev. Comp. Immunol. 42, 323–332.
Yi, G.H., Wang, Z.M., Qi, Y.P., Yao, L.G., Q, J., Hu, L.B., 2004. Vp28 of shrimp white spot syndrome virus is involved in the attachment and penetration into shrimp cells. BMB Rep. 37, 726–734.
Zhang, Y., Qiu, L.M., Song, L.S., Zhang, H., Zhao, J.M., Wang, L.L., Yu, Y.D., Li, C.H., Li, F.M., Xing, K.Z., Huang, B.X., 2009a. Cloning and characterization of a novel C-type lectin gene from shrimp *Litopenaeus vannamei*. Fish Shellfish Immunol. 6, 183–192.
Zhang, X.W., Xu, W.T., Wang, X.W., Mu, Y., Zhao, X.F., Yu, X.Q., Wang, J.X., 2009b. A novel C-type lectin with two CRD domains from Chinese shrimp *Fenneropenaeus chinensis* functions as a pattern recognition protein. Mol. Immunol. 46, 1626–1637.
Zhao, Z.Y., Yin, Z.X., Xu, X.P., Weng, S.P., Rao, X.Y., Dai, Z.X., Luo, Y.W., Yang, G., Li, Z.S., Guan, H.J., Li, S.D., Chan, S.M., Yu, X.Q., He, J.G., 2009. A novel C-type lectin from the shrimp *Litopenaeus vannamei* possesses anti-white spot syndrome virus activity. J. Virol. 83, 347–356.
Zhou, Q., Xu, L.M., Li, H., Qi, Y.P., Yang, F., 2009. Four major envelope proteins of white spot syndrome virus bind to form a complex. J. Virol. 83, 4709–4712.